

<https://helda.helsinki.fi>

---

## Matrix-Isolation and ab Initio Study of HNgCCF and HCCNgF Molecules (Ng = Ar, Kr, and Xe)

Khriachtchev, Leonid

American Chemical Society

2010

---

Khriachtchev , L , Domanskaya , A , Lundell , J , Akimov , A , Räsänen , M & Misochko , E  
2010 , ' Matrix-Isolation and ab Initio Study of HNgCCF and HCCNgF Molecules (Ng = Ar,  
Kr, and Xe) ' , Journal of Physical Chemistry A , vol 114 , no. 12 , pp. 4181-4187 .

---

<http://hdl.handle.net/10138/23938>

<http://dx.doi.org/10.1021/jp1001622>

---

*Downloaded from Helda, University of Helsinki institutional repository.*

*This is an electronic reprint of the original article.*

*This reprint may differ from the original in pagination and typographic detail.*

*Please cite the original version.*

# Matrix-Isolation and *ab Initio* Study of HNgCCF and HCCNgF Molecules (Ng = Ar, Kr, and Xe)

Leonid Khriachtchev,<sup>\*,†</sup> Alexandra Domanskaya,<sup>†</sup> Jan Lundell,<sup>‡</sup> Alexander Akimov,<sup>§</sup> Markku Räsänen,<sup>†</sup> and Eugenii Misochko<sup>§</sup>

Department of Chemistry, University of Helsinki, P.O. Box 55, FIN-00014 Helsinki, Finland, Department of Chemistry, University of Jyväskylä, P.O. Box 35, FIN-40014 Jyväskylä, Finland, and Institute of Problems of Chemical Physics of the Russian Academy of Sciences, 142432 Chernogolovka, Moscow Region, Russia

Received: January 7, 2010; Revised Manuscript Received: February 9, 2010

We report three new noble-gas molecules prepared in low-temperature Kr and Xe matrices from the HCCF precursor by UV photolysis and thermal annealing. The identified molecules are two noble-gas hydrides HNgCCF (Ng = Kr and Xe) and a molecule of another type, HCCrF. These molecules are assigned with the help of *ab initio* calculations. All strong absorptions predicted by theory are found in experiments with proper deuteration shifts. The experiments and theory suggest a higher stability against dissociation of HNgCCF molecules compared to HNgCCH reported previously. Surprisingly, only very tentative traces of HCCXeF, which is computationally very stable, are found in experiments. No strong evidence of similar argon compounds is found here.

## 1. Introduction

The experimental chemistry of noble gases began with a room-temperature synthesis of xenon hexafluoroplatinate (XePtF<sub>6</sub>) by Bartlett in 1962.<sup>1</sup> Many compounds with Xe and Kr atoms have been reported later, XeF<sub>2</sub> and KrF<sub>2</sub> being important for synthetic work.<sup>2–5</sup> The experimentally identified argon compounds are charged species, the exception being the neutral ground-state molecule HArF.<sup>6,7</sup> Additional neutral argon molecules FArCCH and FArSiF<sub>3</sub> were theoretically predicted by Cohen et al.<sup>8</sup> HCCNgCN and HCCNgNC (Ng = Ar, Kr, and Xe) are also computationally stable species; however, the experimental attempts to prepare them failed, whereas HNgCCCN molecules (Ng = Kr and Xe) were identified.<sup>9</sup>

The chemical bonds between a noble gas (Ng) and other atoms are usually quite weak, and examination of noble-gas chemistry benefits greatly from studies by cryogenic techniques.<sup>4,10</sup> Soon after the breakthrough of Bartlett,<sup>1</sup> noble-gas halides like KrF<sub>2</sub>, XeCl<sub>2</sub>, and XeClF were prepared and identified in matrix-isolation experiments.<sup>11,12</sup> The power of matrix isolation was impressively demonstrated by identification of noble-gas hydrides with the general formula HNgY (Ng = Ar, Kr, and Xe; Y = an electronegative fragment).<sup>6,7,10,13–15</sup> A standard procedure for preparing these species includes photodissociation of HY precursors and thermal mobilization of H atoms in noble-gas matrices. At present, 23 noble-gas hydrides are known,<sup>10</sup> including a neutral chemical compound of argon, HArF.<sup>6,7</sup> The latest member of this family of molecules is doubly “xenonated” water, HXeOXeH.<sup>16</sup>

The energetic stability of various noble-gas compounds is of a key importance for the future of this research area and has been repeatedly discussed for the case of noble-gas hydrides.<sup>15,17,18</sup> Noble-gas compounds generated first in low-temperature ma-

trices could lead to an important synthetic value if these species would be realized under ambient conditions. Tsivion et al. predicted that HXeCCH may be stable up to room temperature.<sup>18</sup>

In this work, we report three new noble-gas compounds prepared in low-temperature matrices employing the HCCF precursor to make HCCNgF and HNgCCF molecules. The initial motivation was an attempt to prepare HCCArF predicted by Cohen et al.<sup>8</sup> It was also interesting to compare the HNgCCF noble-gas hydrides with the previously reported HNgCCH species (Ng = Kr and Xe)<sup>19–21</sup> with respect to the energetic stability and in view of the recent prediction of HXeCCH possibly being stable at room temperature.<sup>18</sup>

## 2. Calculations

**Computational Details.** The structural, energetic, and spectroscopic properties of the HNgCCF and HCCNgF molecules were studied by *ab initio* methods utilizing Gaussian 03 revision E.01.<sup>22</sup> The molecular geometries were optimized at the MP2 level of theory using the Dunning-type aug-cc-pVTZ basis set to describe the H, C, F, and Ar atoms.<sup>23,24</sup> For the Kr and Xe atoms, the aug-cc-pVTZ quality valence shell description was combined with Stuttgart small core relativistic effective core potentials,<sup>25</sup> and these ECP-involved basis sets are labeled here as aug-cc-pVTZ-PP. All optimized structures were validated by frequency calculations, indicating that the obtained structures were local minimum structures without imaginary frequencies in their spectra. Both frequencies and IR intensities of the H and D forms of the molecules were studied to assist the experimental work. The partial charges for each atom in the new compounds were calculated through the natural population analysis (NPA).<sup>26</sup> The energetic properties of the new molecules were computed at the MP2 and CCSD(T) levels of theory employing the MP2/aug-cc-pVTZ-PP computed equilibrium structure. In the energy calculations, the CCSD(T)/aug-cc-pVTZ optimized structures of CCH and CCF were used since MP2 calculations of open shell radicals are notorious for yielding wrong energetic and even structural data. Another reference point for our calculations was the structural and spectral

\* To whom correspondence should be addressed. E-mail: leonid.khriachtchev@helsinki.fi.

<sup>†</sup> University of Helsinki.

<sup>‡</sup> University of Jyväskylä.

<sup>§</sup> Institute of Problems of Chemical Physics of the Russian Academy of Sciences.

**TABLE 1: Experimental and Theoretical Vibrational Frequencies of HCCF and DCCF (cm<sup>-1</sup>)<sup>a</sup>**

assignment	theory <sup>b</sup>		experiment <sup>c</sup>									
	HCCF	DCCF	HCCF			DCCF						
			Ar	Kr	Xe	gas <sup>d</sup>	Ne <sup>e,f</sup>	Ar <sup>f</sup>	Kr <sup>f</sup>	Xe <sup>f</sup>	gas <sup>d</sup>	
C–C–F bend	374.8 (2.0)	374.4	–	–	–	367	–	–	–	–	–	364
C–C–H bend	584.4 (42.8)	441.4	583	585, 581w	580, 581	578	–	442	442, 440w	439	–	439
C–F stretch	1071.8 (74.7)	1050.1	1057	1060, 1056w	1058	1055	1046	1042	1045, 1041w	1042.5	–	1048
C=C stretch	2250.5 (129.6)	2115.8	2236.5	2237, 2233w	2233	2255	2114, 2059.5	2108, 2053	2111.5, 2105w, 2057, 2050.5w	2107, 2052	–	2065
C–H stretch	3515.6 (95.9)	2730.3	3349	3355, 3350, 3341w	3345, 3340	3355	2647	2639.5	2642, 2640.5, 2635w	2637.5, 2634.5	–	2645

<sup>a</sup> The computational intensities (in km mol<sup>-1</sup>) are in parentheses. <sup>b</sup> At the MP2/aug-cc-pVTZ level of theory. <sup>c</sup> Weak bands marked with w are probably from HCCF dimers. <sup>d</sup> From ref 31. <sup>e</sup> Only the deuterated species was studied in a Ne matrix. <sup>f</sup> The C=C stretching mode is split due to the Fermi resonance discussed in ref 32.

**TABLE 2: Computational (MP2/aug-cc-pVTZ-PP) Bond Lengths of the HNgCCF and HCCNgF Linear Structures (Å) and Partial Charges (elementary charges)**

	Ar	Kr	Xe
HNgCCF			
<i>r</i> (H–Ng)	1.447	1.552	1.721
<i>r</i> (Ng–C1)	2.175	2.225	2.330
<i>r</i> (C1=C2)	1.227	1.227	1.228
<i>r</i> (C2–F)	1.293	1.292	1.291
<i>q</i> (H)	0.10	0.01	–0.11
<i>q</i> (Ng)	0.44	0.56	0.72
<i>q</i> (C1)	–0.53	–0.59	–0.65
<i>q</i> (C2)	0.28	0.30	0.32
<i>q</i> (F)	–0.28	–0.28	–0.28
HCCNgF			
<i>r</i> (F–Ng)	1.894	1.960	2.065
<i>r</i> (Ng–C1)	1.799	1.903	2.068
<i>r</i> (C1=C2)	1.215	1.216	1.219
<i>r</i> (C2–H)	1.063	1.063	1.063
<i>q</i> (F)	–0.62	–0.66	–0.71
<i>q</i> (Ng)	0.72	0.88	1.07
<i>q</i> (C1)	–0.12	–0.24	–0.38
<i>q</i> (C2)	–0.22	–0.22	–0.22
<i>q</i> (H)	0.24	0.24	0.23

properties of HCCF (see Table 1), and the results are close to the experimental data. The computational approach used here is similar to those used previously in the search for new noble-gas hydrides and has become a useful and cost-effective approach.<sup>10,13,14</sup> All calculations were performed on the computers at the CSC-Center for Scientific Computing Ltd. (Espoo, Finland).

**Computational Results.** True minima are found on the potential energy surfaces of six molecules of HNgCCF and HCCNgF (Ng = Ar, Kr, and Xe). The optimized HNgCCF and HCCNgF molecules have linear structures, and the geometrical parameters are listed in Table 2. All these molecules exhibit a strong charge-transfer character. In the noble-gas hydrides HNgCCF, the H–Ng part is positively charged, the charge increasing from Ar to Kr and Xe, and the CCF part is negatively charged. This is in accord with the general view of the H–Ng bond being predominantly covalent and the Ng–C bond being mainly ionic.<sup>10</sup> In the HCCNgF molecules, the Ng atom is positively charged (up to +1.07e for Xe) whereas F and CCH carry negative charges. In this case, the bonding pattern is similar to the case of F–Xe–F in which a delocalized bonding over the three centers appears and both F–Xe bonds reflect ionic contributions.

The computational vibrational frequencies of HNgCCF and HCCNgF molecules and their deuterated analogues are collected in Table 3. For the noble-gas hydrides HNgCCF, the H–Ng stretching mode is very strong (>10<sup>3</sup> km mol<sup>-1</sup>), which is a

characteristic feature of all known noble-gas hydrides. The calculated H–Ng stretching frequencies are 1371, 1694, and 1759 cm<sup>-1</sup> when Ng = Ar, Kr, and Xe, respectively. It should be stressed that the H–Ar stretching frequency of HARCCF is very low compared to that of HARF (~2000 cm<sup>-1</sup>),<sup>27</sup> which raises doubts about its practical stability. When considering the H–Ng stretching modes, one should keep in mind that their frequencies are, as a rule, overestimated by the harmonic theory used here.<sup>13</sup> The C=C and C–F stretching modes of HNgCCF with an intensity of ~100 km mol<sup>-1</sup> are also detectable, whereas other vibrational intensities are much weaker. For the HCCNgF molecules, the strongest absorption originates from the Ng–F stretching mode (several hundreds of kilometers per mole), and the other observable absorptions belong to the C=C and C–H stretching modes and the CCH bending mode. The intense Ng–C stretching absorption appears below the frequency range accessible in these experiments.

The predicted noble-gas molecules are metastable species that are above the Ng + HCCF global energy minimum by several electronvolts (two-body decomposition channel, 2B) (see Table 4). The lowest in energy is HCCXeF that is higher than the Xe + HCCF asymptote by “only” 2.78 eV. The HNgCCF and HCCNgF molecules (Ng = Kr and Xe) are reliably lower in energy than the H + Ng + CCF and HCC + Ng + F fragments, respectively (three-body decomposition channel, 3B), which ensures their low-temperature stability and enables the annealing-promoted formation. The most stable species, HCCXeF, is lower in energy than the HCC + Ng + F asymptote by 2.86 eV. HNgCCF molecules (Ng = Kr and Xe) have a slightly larger 3B dissociation energy than HNgCCH reported previously (see refs 19–21) (by ca. 0.06 eV at the same level of theory). HCCArF is computationally only 0.14 eV below the 3B asymptote, whereas HARCCF is 0.44 eV above the 3B asymptote. In the case of HCCArF, the energy difference is diminished by 30% when zero-point energies are taken into account; i.e., the molecular energy becomes closer to the dissociation energy limit.

The accuracy of the computed energies can be estimated via comparison of experimental and computational dissociation energies of the precursor.<sup>28</sup> Indeed, the position of the 3B asymptote with respect to the noble-gas molecule is of crucial importance for the low-temperature formation mechanism. The calculated energy for dissociation of HCCH to H and CCH at the present level of theory is ca. 6.0 eV, which is ca. 0.3 eV larger than the experimental value.<sup>29</sup> The experimental HCCF dissociation energy is not available, but a similar uncertainty in the energetics of the corresponding system exists in this case as well. Most probably the energetic stability of the predicted noble-gas molecules is overestimated by the present computa-

**TABLE 3: Computational Vibrational Frequencies (in  $\text{cm}^{-1}$ ) and Absorption Intensities ( $\text{km mol}^{-1}$  in parentheses) of H(D)NgCCF and H(D)CCNgF at the MP2/aug-cc-pVTZ-PP Level of Theory**

assignment <sup>a</sup>	Ar molecules		Kr molecules		Xe molecules	
	H	D	H	D	H	D
	H(D)NgCCF					
	58.3 (18.9)	56.6 (17.2)	88.8 (13.3)	86.6 (12.4)	85.5 (8.7)	83.3 (8.1)
	279.3 (297.0)	279.3 (294.5)	261.5 (148.0)	261.4 (147.4)	244.4 (123.9)	244.4 (123.7)
	352.0 (0.4)	351.7 (0.4)	367.0 (0.6)	365.9 (0.5)	371.8 (0.4)	370.4 (0.2)
	734.2 (5.6)	546.5 (0.7)	722.9 (0.9)	532.7 (0.0)	675.0 (2.6)	496.4 (3.2)
C–F stretch	1073.8 (76.1)	1074.8 (7.9)	1081.0 (31.1)	1081.0 (27.5)	1083.6 (21.6)	1083.4 (16.3)
H–Ng stretch	1370.7 (3915.4)	974.9 (2071.9)	1694.2 (1939.8)	1203.5 (1000.6)	1759.4 (1157.3)	1248.4 (596.2)
C=C stretch	2175.1 (162.6)	2174.6 (133.0)	2175.1 (193.9)	2174.9 (174.9)	2171.7 (33.7)	2171.7 (221.0)
	H(D)CCNgF					
	104.6 (0.7)	100.2 (0.9)	120.1 (1.3)	115.1 (1.4)	119.2 (1.6)	114.6 (1.5)
	351.5 (14.5)	349.7 (15.9)	340.2 (16.4)	333.3 (18.6)	316.3 (20.4)	308.4 (22.3)
	372.2 (153.4)	366.4 (148.9)	428.0 (55.9)	420.2 (55.4)	433.9 (62.5)	425.4 (58.8)
Ng–F stretch	545.4 (513.6)	545.3 (510.7)	510.3 (318.3)	510.2 (314.9)	488.2 (238.9)	488.2 (239.9)
C–C–H bend	653.2 (37.1)	503.1 (16.8)	651.0 (36.5)	507.7 (14.4)	660.4 (37.4)	515.6 (14.6)
C=C stretch	2042.3 (66.7)	1918.9 (98.2)	2048.0 (27.0)	1924.5 (47.4)	2034.3 (14.0)	1913.8 (28.8)
C–H stretch	3476.1 (86.2)	2676.2 (25.6)	3474.3 (79.2)	2674.8 (30.4)	3470.2 (73.5)	2668.8 (32.6)

<sup>a</sup> Assignments of the experimentally observed bands are presented.

**TABLE 4: Computational Energy (eV) of HNgCCF(H) and HCCNgF Molecules ( $E_m$ ) with Respect to the Energy of the H + Ng + CCF(H) and HCC + Ng + F Fragments ( $E_f$ ) and the Ng + HCCF(H) Global Minimum ( $E_g$ )<sup>a</sup>**

	$E_f - E_m$	$E_g - E_m$
HCCArF	0.14	-5.50
HCCKrF	1.56	-4.08
HCCXeF	2.86	-2.78
HArCCF	-0.44	-6.46
HKrCCF	0.62	-5.40
HXeCCF	1.48	-4.53
HKrCCH	0.56	-5.46
HXeCCH	1.42	-4.59

<sup>a</sup> Computed at the CCSD(T)/aug-cc-pVTZ-PP//MP2/aug-cc-pVTZ-PP level using energies of optimized molecular structures of CCH and CCF at the CCSD(T)/aug-cc-pVTZ level.

tional method as discussed elsewhere.<sup>28</sup> Because of this uncertainty, we cannot claim the stability of HCCArF with respect to the 3B asymptote, and more extensive theoretical work is required to address this issue.

The metastable HNgCCF and HCCNgF species are kinetically stabilized via the bending coordinate by an energy barrier. The bending barrier exhibits a single-configuration nature, and MP2 optimizations of the transition state along this energy barrier yield values of 1.93 and 2.86 eV for HXeCCF and FXeCCH, respectively, compared to the computed molecular energies. Therefore, the 3B dissociation channel is presumably more important for the stability of these molecules than the dissociation process via the bending coordinate.<sup>10,13</sup> The 3B (stretching) barrier leading to the H + Ng + CCF and HCC + Ng + F fragments is more difficult to evaluate because this requires very time-consuming multiconfigurational methods. This complicated analysis was conducted for the HXeCCH and HArF molecules.<sup>18,27</sup> At low temperatures, the 3B barrier is not of primary importance for the stability of molecules that are lower in energy than the reacting fragments (as the reliable case here for Ng = Kr and Xe). On the other hand, a high stretching barrier can in principle prevent the formation of noble-gas molecules from the neutral fragments at low temperatures.

### 3. Experiment

**Experimental Details.** The HCCF/Ng (Ng = Ar, Kr, and Xe) matrices with typical ratios of 1/2000 to 1/1000 and a

thickness of 100  $\mu\text{m}$  were deposited onto a cold CsI substrate at temperatures from 10 to 35 K (depending on the matrix material) in a closed-cycle helium cryostat (APD, DE 202A, temperature down to 9 K). The IR absorption spectra in the 4000–400  $\text{cm}^{-1}$  range were recorded with a Bruker Vertex 80 FTIR spectrometer with a resolution of 0.5  $\text{cm}^{-1}$  co-adding 200–500 scans. The matrices were photolyzed with a 193 nm excimer laser (MPB, MSX-250, pulse energy density of  $\sim 10$   $\text{mJ cm}^{-2}$ ), and VUV light from krypton and xenon lamps (Optos). The photolyzed matrices were annealed, and the IR spectra were measured at 9 K. The experiments in a Ne matrix were performed at 4.2 K using a Sumitomo Heavy Industries cryostat and a Nicolet SX60 FTIR spectrometer (resolution of 0.5  $\text{cm}^{-1}$ ).

HCCF (DCCF) was prepared by direct-current glow discharge decomposition of 1,3,5-trifluorobenzene in a helium atmosphere.<sup>30</sup> During the synthesis, the discharge products were collected in a liquid nitrogen trap. HCCF (DCCF) was purified by a trap-to-trap distillation employing a liquid nitrogen/2-methylbutane slush bath at  $-150$  °C. Nondeuterated 1,3,5-trifluorobenzene (98+%, CAS Registry Number 372-38-3) was purchased from Alfa Aesar. 1,3,5-Trifluorobenzene was deuterated when it was mixed with concentrated  $\text{D}_2\text{SO}_4$  for 2–3 h at room temperature followed by a trap-to-trap distillation in a vacuum line. The process was repeated four times to produce the desired degree of deuteration (ca. 96%).

**Experimental Results.** After deposition, the noble-gas matrices contain mainly monomeric HCCF (DCCF), and the assignment is straightforward on the basis of the gas-phase data.<sup>31,32</sup> The IR spectra of HCCF and DCCF in a Kr matrix are shown in Figure 1. Reasonably small amounts of acetylene, water,  $\text{CO}_2$ , and  $\text{CHF}_3$  are present in the matrices as impurities. The frequencies of the HCCF fundamental vibrations in various matrices (Ne, Ar, Kr, and Xe) together with our computational results are collected in Table 1.

Typically,  $\sim 60\%$  of HCCF is decomposed in these experiments (Ng = Ar, Kr, and Xe), and further decomposition is probably limited by photolysis-induced absorbers (self-limited photolysis).<sup>33</sup> The UV photolysis of HCCF leads to a number of products. The IR-active photolysis products include NgHN $\text{g}^+$ ,<sup>34,35</sup> CCH radicals (e.g., 1842  $\text{cm}^{-1}$  in a Kr matrix),<sup>21</sup> and HF in the monomeric and complexed forms (probably with CC). In a Xe matrix, the

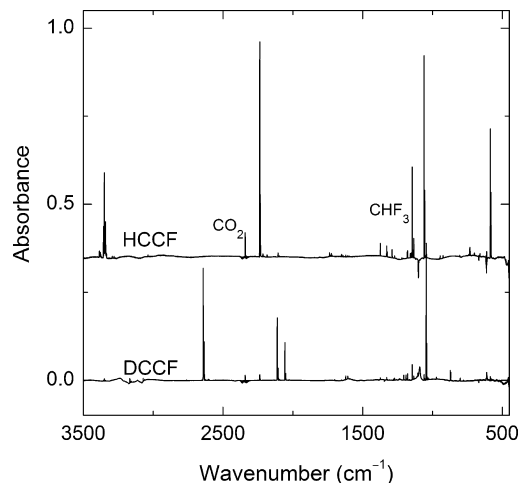


**Figure 1.** HCCF and DCCF in a Kr matrix at 9 K. Some of the broad and negative peaks arise from the spectrum background.

**TABLE 5: Experimental Frequencies ( $\text{cm}^{-1}$ ) of HNgCCF and HCCNgF Molecules (Ng = Kr and Xe)**

assignment	HNgCCF <sup>a</sup>	
	Kr	Xe
C–F stretch	1051 (1051)	1054 (1054)
H(D)–Ng stretch	1384 (1010)	1548 (1121.5)
C=C stretch	2177 (2178)	2171 (2169)
assignment	HCCNgF <sup>a</sup>	
	Kr	Xe <sup>b</sup>
F–Ng stretch	468 (468)	–
C–C–H bend	653 (506)	–
C=C stretch	2058 (1922)	–
C–H stretch	3299 (2588)	–

<sup>a</sup> Values in parentheses are for deuterated species DNgCCF and DCCNgF. <sup>b</sup> Assignment of the band at  $2050.5 \text{ cm}^{-1}$  to the C=C stretching mode of HCCXeF is not supported by additional observations. A similar band at 2065 and  $2071 \text{ cm}^{-1}$  may in principle belong to HCCArF, but no additional experimental support is available.

Xe–CC molecules exhibit a strong peak at  $1767 \text{ cm}^{-1}$ .<sup>36</sup> One photolysis product, which has not been reported experimentally to the best of our knowledge, has a structured absorption around  $1600 \text{ cm}^{-1}$  in Ar, Kr, and Xe matrices. On the basis of the experimental evidence, we tentatively assign this absorption to the CCF radical. HFCC is another candidate for this absorption; however, the observed bands remain practically unchanged after deuteration, which makes this assignment improbable. A number of other broad and less intense absorptions are seen in the spectra, probably belonging to different radicals (including CCH<sup>37</sup> and CCF) and ionic species. The best yield of the key products was obtained with Xe lamp photolysis. Photolysis of a DCCF/Ne matrix does not lead to noticeable decomposition of DCCF, and the band around  $1600 \text{ cm}^{-1}$  does not appear.

Annealing of the photolyzed matrices up to 30 K (Kr) and 45 K (Xe) leads to a number of products, including three previously unknown noble-gas compounds. The vibrational frequencies of these new noble-gas molecules (HKrCCF, HCCrF, and HXeCCF) are collected in Table 5. The formation process in a Kr matrix is illustrated in Figure 2. The other annealing products in a Xe matrix include noble-gas species HXeH,<sup>38</sup> XeF<sub>2</sub> (at  $542 \text{ cm}^{-1}$ ) in small amounts,<sup>39</sup> HXeCCH, HXeCC, minor traces of HXeCCXeH,<sup>19</sup> and HXeOH (from water impurity).<sup>40</sup> In a Kr matrix, HKrF (stable configuration)

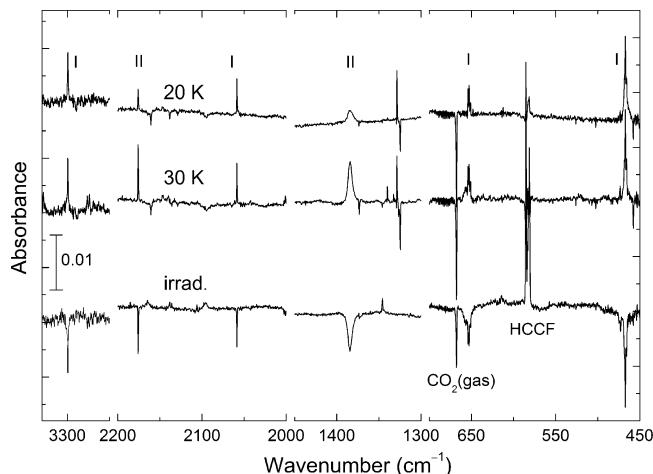


**Figure 2.** HCCrF (I) and HKrCCF (II) in a Kr matrix at 9 K. Shown from top to bottom are the spectra after annealing at 20 K, annealing at 30 K, and the result of short irradiation at 193 nm. The HCCF/Kr ( $\sim 1/1000$ ) matrices were preliminarily photolyzed by a Xe lamp for  $\sim 1 \text{ h}$ .

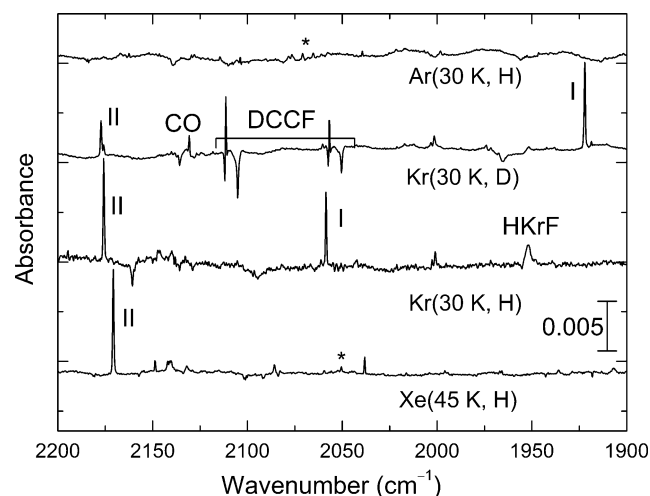


**Figure 3.** Deuteration and matrix effects on the annealing-produced spectra. Shown from top to bottom are the difference spectra in an Ar matrix, in a Kr matrix (from DCCF), in a Kr matrix (from HCCF, already shown in Figure 2), and in a Xe matrix presenting the result of annealing (annealing temperatures are marked). The H(D)CCF/Ng matrices were preliminarily photolyzed with a Xe lamp. The weak bands marked with an asterisk may be from the HCCNgF (Ng = Ar and Xe) species; however, no additional support of this assignment is available. The notations HCCr(Xe)F (I) and HKrCCF (II) are used.

is observed in small amounts at  $1952 \text{ cm}^{-1}$ ,<sup>41</sup> as well as minor traces of HKrCCH.<sup>21</sup> The NgHNg<sup>+</sup> (Ng = Kr and Xe) concentration decreases upon annealing. In experiments with DCCF, all the corresponding deuterated species appear. Unfortunately, no bands that could definitely be assigned to argon compounds HArCCF and HCCArF were found in the spectra in the HCCF/Ar matrix experiments (see Figure 3).

The bands of noble-gas molecules are easily bleached by UV light, which is a useful property for their assignment.<sup>42</sup> We performed this post-annealing bleaching using different exposures to 193 nm light. Upon 193 nm irradiation of the annealed matrices, the bands belonging to CCH, CCF (tentatively), and HCCF rise together with the decomposition of the assigned noble-gas species. HXeCC is efficiently decomposed by the spectrometer IR light, whereas the newly observed noble-gas species are quite stable upon this irradiation. The thermal stabilities of HXeCCH and HXeCCF are found to be comparable

as checked by annealing at 70 K. Upon annealing at 70 K, the band assigned to the H–Xe stretching mode of HXeCCF is substantially narrowed.

#### 4. Discussion and Conclusions

**Assignment of the Kr Compounds.** In a HCCF/Kr matrix, two sets of bands are found in the IR spectra after UV photolysis and annealing, and they are assigned to the HKrCCF and HCCKrF molecules (see Table 5). The separation of these two absorbers is experimentally straightforward. The bands assigned to HCCKrF are formed already during UV photolysis and reach the maximum intensity upon annealing at ca. 20 K. The bands assigned to HKrCCF are not present after photolysis; they partially build up at 20 K and reach their maximum intensity at ~30 K. None of these bands appear in the corresponding experiments in an Ar matrix (with normal matrix shifts), which strongly points to the Kr compounds. As additional support, these bands are characteristically bleached by UV light.

All strong bands computationally predicted for these krypton compounds are observed in experiments. The H–Kr stretching frequency is computationally overestimated ( $1694\text{ cm}^{-1}$  vs  $1384\text{ cm}^{-1}$ ); however, this is typical for noble-gas hydrides described in the harmonic approximation.<sup>13</sup> For HKrCCF and HCCKrF, three and four fundamental modes, respectively, are observed in the experimental spectra, properly behaving upon deuteration. The shift of the C=C stretching band is a good fingerprint. For DKrCCF, the C=C stretching shift is very small ( $\sim 1\text{ cm}^{-1}$ ), which agrees with theory. For DCCKrF, the C=C stretching shift is  $-136\text{ cm}^{-1}$ , agreeing well with the theoretical value of  $-124\text{ cm}^{-1}$ . The H–Kr stretching mode shifts upon deuteration from  $1384$  to  $1010\text{ cm}^{-1}$ , which shows a proper H/D frequency ratio of 1.370.

The following formation mechanism of HKrCCF and HCCKrF is suggested. The photolysis products of HCCF are likely the  $\text{H} + \text{CCF}$ ,  $\text{HCC} + \text{F}$ ,  $\text{H} + \text{CC} + \text{F}$ , and  $\text{HF} + \text{CC}$  fragments. Some HCCKrF molecules are formed upon photolysis due to the short-range escape of F atoms.<sup>42</sup> The additional formation of HCCKrF occurs at 20 K in the  $\text{HCC} + \text{Kr} + \text{F}$  reaction due to the mobility of F atoms. In accord, the CCH concentration decreases upon annealing at 20 K. Pettersson et al. reported that global mobility of F atoms is activated in a Kr matrix above 20 K,<sup>41</sup> which favors the local process in our case because most of the HCCKrF molecules are formed below 20 K. The formation of HKrCCF takes place presumably in the  $\text{H} + \text{Kr} + \text{CCF}$  reaction upon global mobility of H atoms at ca. 30 K, as for other Kr-containing hydrides.<sup>43</sup> At this temperature, the broad band around  $1600\text{ cm}^{-1}$  decreases, which is consistent with our tentative assignment of this absorption to CCF. Upon annealing, CCH and CCF radicals can be formed in some amounts in the  $\text{CC} + \text{H}$  and  $\text{CC} + \text{F}$  reactions, but the proportion of these channels is difficult to estimate. The formation of CCF could be in principle suppressed if CCKrF radical was formed, but we could see no evidence of this open-shell species. To remind ourselves, HKrCC was reported to be an unstable species.<sup>21</sup>

**Assignment of the Xe Compound.** In a HCCF/Xe matrix, the HXeCCF species is identified in the IR spectra after UV photolysis and annealing at ca. 40 K. The C=C and C–F stretching bands of HXeCCF appear close to those of HKrCCF, the relative shifts being in good agreement with the calculations. The experimental H–Xe stretching band of HXeCCF is substantially higher in energy ( $1548\text{ cm}^{-1}$ ) than the H–Kr stretching band of HKrCCF ( $1384\text{ cm}^{-1}$ ), which is also observed for the Xe/Kr pairs of other noble-gas hydrides such as HNgCl,<sup>44</sup>

HNgCN,<sup>45</sup> HNgC<sub>3</sub>N,<sup>9</sup> HNgCCH,<sup>19–21</sup> and HNgC<sub>4</sub>H.<sup>46</sup> The D–Xe stretching band of DXeCCF shifts upon deuteration from  $1548$  to  $1121.5\text{ cm}^{-1}$ , which features a proper H/D frequency ratio of 1.380. It is worth noting that the absorption of DXeCCF is very close to one of the HXeD bands;<sup>38</sup> however, the analysis shows a negligible contribution of the HXeD absorption to the  $1121.5\text{ cm}^{-1}$  band of DXeCCF. The formation of HXeCCF occurs via the  $\text{H} + \text{Xe} + \text{CCF}$  reaction presumably controlled by global mobility of hydrogen atoms activated at ca. 40 K,<sup>47</sup> which is similar to HXeCCH and HXeCC formation.

No conclusive evidence for formation of HCCXeF is found in these experiments (see Figure 3). A very weak band at  $2050\text{ cm}^{-1}$  may belong to this species (C=C stretching mode) because it rises upon annealing and is easily bleached by UV irradiation. However, other bands of the same species and the corresponding band of the deuterated species are not found in the spectra. It is important to note in this context that the computationally stable HXeF species<sup>48</sup> has not been experimentally found, whereas the less stable HARF and HKrF molecules have been prepared.<sup>6,7,41</sup> We have no doubts about the computational energetic stability of this molecule (see Table 4) and about the presence of the F and CCH fragments in the matrix, and other reasons are responsible for the lack of formation of HCCXeF. It is probable that the reactivity and mobility of F atoms in a Xe matrix are suppressed by the strong Xe–F interaction ( $145\text{ meV}$ ).<sup>49</sup> As another possibility, the bending stabilization barrier of HCCXeF and HXeF can in principle be lowered in a Xe matrix, which is similar to a destabilization effect found computationally for HXeOH in water clusters by Nemukhin et al.<sup>17</sup>

**CCF Radical.** The formation of HKrCCF and HXeCCF requires the presence of CCF radicals in the matrix after the photolysis. CCF is a likely photolysis product of HCCF, and we tentatively assign the broad structured band around  $1600\text{ cm}^{-1}$  to CCF. The properties of the CCF radical have been computationally studied by Tarroni; unfortunately, his data provide no explicit vibrational spectrum (with intensities), and they cannot be used here for identification of the radical.<sup>50</sup> We calculated the CCF radical at the CCSD(T)/aug-cc-pVTZ level of theory and obtained a slightly bent structure ( $158.1^\circ$ ) with C–F and C–C distances of  $1.2754$  and  $1.2775\text{ \AA}$ , respectively, which are consistent with the values obtained by Tarroni ( $165^\circ$ ,  $1.276\text{ \AA}$ , and  $1.271\text{ \AA}$ , respectively). The CCSD(T) vibrational frequencies of CCF are  $404.9$ ,  $1009.1$ , and  $1706.8\text{ cm}^{-1}$ . The CCH radical at the same level of theory has frequencies of  $379.8$ ,  $2048.7$ , and  $3451.5\text{ cm}^{-1}$ . The computational CCH frequency of  $2048.7\text{ cm}^{-1}$  should be compared to the frequency of  $1842\text{ cm}^{-1}$  for the C=C stretching absorption in a Kr matrix. In this situation, the C=C stretching absorption of CCF at ca.  $1600\text{ cm}^{-1}$  looks reasonable (computationally  $1706.8\text{ cm}^{-1}$ ) because the scaling factor would be very similar. However, we should admit that this computational method is not suitable for describing open-shell species because of the probable contribution of a number of other states.<sup>50</sup> More computational efforts are required for reliable assignment of CCF, which exceeds the scope of this work focusing on noble-gas species.

**Comparison with Other Noble-Gas Compounds.** It is worth noting that HKrCCF and HXeCCF are conventional noble-gas hydrides, which increases their number to 25,<sup>10</sup> whereas HCCKrF belongs to another group appearing in this kind of experiments for the first time. In matrix-isolation experiments, ClXeF is probably the closest example to HCCKrF,<sup>12</sup> and no such Kr compounds have been previously reported to the best of our knowledge. Similar HCCNgCN molecules (Ng = Ar, Kr, and Xe) were computationally predicted but did not form

in experiments.<sup>9</sup> The difference may be in the higher mobility of F atoms in solid krypton compared to CN radicals.

The new hydrides HKrCCF and HXeCCF are analogues of known HKrCCH and HXeCCH, respectively.<sup>19–21</sup> Our data suggest the energetic stabilization of the HNgCCF species compared to HNgCCH. This is evidenced by the experimental H–Ng stretching bands that are at 1384 and 1548 cm<sup>-1</sup> for HKrCCF and HXeCCF, respectively, whereas they are at lower frequencies (1241.5 and 1486 cm<sup>-1</sup>) for HKrCCH and HXeCCH, respectively. The experimental H/D frequency ratio is 1.370 (Kr) and 1.380 (Xe) for HNgCCF versus 1.287 (Kr) and 1.379 (Xe) for HNgCCH featuring more harmonic vibrations for HNgCCF. The computational H–Ng bond lengths and (HNg) charges are 1.552 Å and +0.57e (Kr) and 1.721 Å and +0.61e (Xe) for HNgCCF compared to 1.574 Å and +0.53e (Kr) and 1.734 Å and +0.58e (Xe) for HNgCCH, featuring stabilization of the H–Ng bond and additional charge separation in the HNgCCF species. The computational energetics supports these stabilization trends for the 3B dissociation channel (see Table 4). The 2B channels computed for HXeCCH and HXeCCF have high barriers (ca. 2.0 eV), and they do not limit the stability of these molecules.

The hypothetically higher stability of HXeCCF compared to that of HXeCCH is noteworthy. Tsivion et al. via computation found that HXeCCH could be stable up to room temperature in the gas phase.<sup>18</sup> Sheng and Gerber predicted crystals composed of HXeCCH molecules.<sup>51</sup> Domanskaya et al. reported complexes of HXeCCH with acetylene in a Xe matrix (stable at least up to 95 K), making a step toward preparation of the noble-gas hydride in an organic host.<sup>52</sup> Similar studies of HXeCCF are clearly interesting taking into account the probable stabilization of this fluorinated species compared to HXeCCH. Furthermore, the computational dissociation energy of HCCrF is 1.56 eV (3B channel), which is 0.14 eV higher than that of HXeCCH. Following speculation by Tsivion et al.,<sup>18</sup> HCCrF may be similarly found in the gas phase.

**How about the Argon Compound?** Argon compound HCCArF is not identified in these experiments despite the expectations. We observed a doublet at 2065 and 2071 cm<sup>-1</sup> after photolysis and annealing at 20 K of a HCCF/Ar matrix which might in principle belong to this argon species. In addition, these bands are easily decomposed by UV light, which is characteristic for noble-gas compounds. However, the intense bands predicted by calculations in other regions as well as the corresponding DCCArF bands (see Table 3) are not found in the spectra, so we cannot suggest this assignment. The reason for the experimental absence of HCCArF may be the lack of energetic stability of this species (see Table 4) or/and the high formation barrier. The computational predictions of noble-gas species should be considered with extreme caution,<sup>28</sup> and this question should be addressed in future work. It is also possible that the H + CCF channel dominates in the HCCF photolysis in solid argon and/or F atoms are immobile upon annealing, preventing the formation of FArCCH. In any case, the experimental identification of the second neutral molecule with argon (after HArF) remains a strong challenge.

**Acknowledgment.** This work was supported by the Academy of Finland through the Finnish Centre of Excellence in Computational Molecular Science and INTAS Project 05-1000008-8017. A.D. acknowledges a postdoctoral grant from the Faculty of Science of the University of Helsinki (Project 7500101). CSC-Center for Scientific Computing Ltd. (Espoo, Finland) is thanked for computer resources.

## References and Notes

- (1) Bartlett, N. *Proc. Chem. Soc., London* **1962**, 218.
- (2) Brel, V. K.; Pirgulyev, N. S.; Zefirov, N. S. *Uspekhi Khimii* **2001**, *70*, 262.
- (3) Lehmann, J. F.; Mercier, H. P. A.; Schrobilgen, G. J. *Coord. Chem. Rev.* **2002**, *233*, 1.
- (4) Grochala, W. *Chem. Soc. Rev.* **2007**, *36*, 1632.
- (5) Misochko, E. Y.; Akimov, A. V.; Belov, V. A.; Tyurin, D. A. *Inorg. Chem.* **2009**, *48*, 8723.
- (6) Khriachtchev, L.; Pettersson, M.; Runeberg, N.; Lundell, J.; Räsänen, M. *Nature* **2000**, *406*, 874.
- (7) Khriachtchev, L.; Pettersson, M.; Lignell, A.; Räsänen, M. *J. Am. Chem. Soc.* **2001**, *123*, 8610.
- (8) Cohen, A.; Lundell, J.; Gerber, R. B. *J. Chem. Phys.* **2003**, *119*, 6415.
- (9) Khriachtchev, L.; Lignell, A.; Tanskanen, H.; Lundell, J.; Kiljunen, H.; Räsänen, M. *J. Phys. Chem. A* **2006**, *110*, 11876.
- (10) Khriachtchev, L.; Räsänen, M.; Gerber, R. B. *Acc. Chem. Res.* **2009**, *42*, 183.
- (11) Turner, J. J.; Pimentel, G. C. *Science* **1963**, *180*, 974.
- (12) Howard, W. F.; Andrews, L. *J. Am. Chem. Soc.* **1974**, *96*, 7864.
- (13) Lundell, J.; Khriachtchev, L.; Pettersson, M.; Räsänen, M. *Low Temp. Phys.* **2000**, *26*, 680.
- (14) McDowell, S. A. C. *Curr. Org. Chem.* **2006**, *10*, 791.
- (15) Lignell, A.; Khriachtchev, L. *J. Mol. Struct.* **2008**, *889*, 1.
- (16) Khriachtchev, L.; Isokoski, K.; Cohen, A.; Räsänen, M.; Gerber, R. B. *J. Am. Chem. Soc.* **2008**, *130*, 6114.
- (17) Nemukhin, A. V.; Grigorenko, B. L.; Khriachtchev, L.; Tanskanen, H.; Pettersson, M.; Räsänen, M. *J. Am. Chem. Soc.* **2002**, *124*, 10706.
- (18) Tsivion, E.; Zilberg, S.; Gerber, R. B. *Chem. Phys. Lett.* **2008**, *460*, 23.
- (19) Khriachtchev, L.; Tanskanen, H.; Lundell, J.; Pettersson, M.; Kiljunen, H.; Räsänen, M. *J. Am. Chem. Soc.* **2003**, *125*, 4696.
- (20) Feldman, V. I.; Sukhov, F. F.; Orlov, A. Y.; Tyulpina, I. V. *J. Am. Chem. Soc.* **2003**, *125*, 4698.
- (21) Khriachtchev, L.; Tanskanen, H.; Cohen, A.; Gerber, R. B.; Lundell, J.; Pettersson, M.; Kiljunen, H.; Räsänen, M. *J. Am. Chem. Soc.* **2003**, *125*, 6876.
- (22) Frisch, M. J.; Trucks, G. W.; Schlegel, H. B.; Scuseria, G. E.; Robb, M. A.; Cheeseman, J. R.; Montgomery, J. A., Jr.; Vreven, T.; Kudin, K. N.; Burant, J. C.; Millam, J. M.; Iyengar, S. S.; Tomasi, J.; Barone, V.; Mennucci, B.; Cossi, M.; Scalmani, G.; Rega, N.; Petersson, G. A.; Nakatsuji, H.; Hada, M.; Ehara, M.; Toyota, K.; Fukuda, R.; Hasegawa, J.; Ishida, M.; Nakajima, T.; Honda, Y.; Kitao, O.; Nakai, H.; Klene, M.; Li, X.; Knox, J. E.; Hratchian, H. P.; Cross, J. B.; Bakken, V.; Adamo, C.; Jaramillo, J.; Gomperts, R.; Stratmann, R. E.; Yazyev, O.; Austin, A. J.; Cammi, R.; Pomelli, C.; Ochterski, J. W.; Ayala, P. Y.; Morokuma, K.; Voth, G. A.; Salvador, P.; Dannenberg, J. J.; Zakrzewski, V. G.; Dapprich, S.; Daniels, A. D.; Strain, M. C.; Farkas, O.; Malick, D. K.; Rabuck, A. D.; Raghavachari, K.; Foresman, J. B.; Ortiz, J. V.; Cui, Q.; Baboul, A. G.; Clifford, S.; Cioslowski, J.; Stefanov, B. B.; Liu, G.; Liashenko, A.; Piskorz, P.; Komaromi, I.; Martin, R. L.; Fox, D. J.; Keith, T.; Al-Laham, M. A.; Peng, C. Y.; Nanayakkara, A.; Challacombe, M.; Gill, P. M. W.; Johnson, B.; Chen, W.; Wong, M. W.; Gonzalez, C.; Pople, J. A. *Gaussian 03*, revision E.012; Gaussian Inc.: Wallingford, CT, 2004.
- (23) Dunning, T. H., Jr. *J. Chem. Phys.* **1989**, *90*, 1007.
- (24) Woon, D. E.; Dunning, T. H., Jr. *J. Chem. Phys.* **1993**, *98*, 1358.
- (25) Peterson, K. A.; Figgen, D.; Goll, E.; Stoll, H.; Dolg, M. *J. Chem. Phys.* **2003**, *119*, 11113.
- (26) Glendening, E. D.; Reed, A. E.; Carpenter, J. E.; Weinhold, F. *NBO*, version 3.1.
- (27) Runeberg, N.; Lundell, J.; Khriachtchev, L.; Pettersson, M.; Räsänen, M. *J. Chem. Phys.* **2001**, *114*, 836.
- (28) Lignell, A.; Khriachtchev, L.; Lundell, J.; Tanskanen, H.; Räsänen, M. *J. Chem. Phys.* **2006**, *125*, 184514.
- (29) Shi, Y.; Ervin, K. M. *Chem. Phys. Lett.* **2000**, *318*, 149.
- (30) Dore, L.; Mazzavillani, A.; Cludi, L.; Cazzoli, G. *J. Mol. Spectrosc.* **1998**, *189*, 224.
- (31) Hunt, G. R.; Wilson, M. K. *J. Chem. Phys.* **1961**, *34*, 1301.
- (32) Anttila, R.; Huhantti, M. *J. Mol. Spectrosc.* **1975**, *54*, 64.
- (33) Khriachtchev, L.; Pettersson, M.; Räsänen, M. *Chem. Phys. Lett.* **1998**, *288*, 727.
- (34) Milligan, D. E.; Jacox, M. E. *J. Mol. Spectrosc.* **1973**, *46*, 460.
- (35) Karatun, A. A.; Sukhov, F. F.; Slovokhotova, N. A. *High Energy Chem.* **1981**, *15*, 371.
- (36) Maier, G.; Lautz, C. *Eur. J. Org. Chem.* **1998**, 769.
- (37) Forney, D.; Jacox, M. E.; Thompson, W. E. *J. Mol. Spectrosc.* **1995**, *170*, 178.
- (38) Pettersson, M.; Lundell, J.; Räsänen, M. *J. Chem. Phys.* **1995**, *103*, 205.
- (39) Smith, D. F. *J. Chem. Phys.* **1963**, *38*, 270.

- (40) Pettersson, M.; Khriachtchev, L.; Lundell, J.; Räsänen, M. *J. Am. Chem. Soc.* **1999**, *121*, 11904.
- (41) Pettersson, M.; Khriachtchev, L.; Lignell, A.; Räsänen, M.; Bihary, Z.; Gerber, R. B. *J. Chem. Phys.* **2002**, *116*, 2508–2515.
- (42) Khriachtchev, L.; Pettersson, M.; Lundell, J.; Räsänen, M. *J. Chem. Phys.* **2001**, *114*, 7727.
- (43) Khriachtchev, L.; Saarelainen, M.; Pettersson, M.; Räsänen, M. *J. Chem. Phys.* **2003**, *118*, 6403.
- (44) Pettersson, M.; Lundell, J.; Räsänen, M. *J. Chem. Phys.* **1995**, *102*, 6423.
- (45) Pettersson, M.; Lundell, J.; Khriachtchev, L.; Räsänen, M. *J. Chem. Phys.* **1998**, *109*, 618.
- (46) Tanskanen, H.; Khriachtchev, L.; Lundell, J.; Kiljunen, H.; Räsänen, M. *J. Am. Chem. Soc.* **2003**, *125*, 16361.
- (47) Khriachtchev, L.; Tanskanen, H.; Pettersson, M.; Räsänen, M.; Feldman, V.; Sukhov, F.; Orlov, A.; Shestakov, A. F. *J. Chem. Phys.* **2002**, *116*, 5708.
- (48) Lundell, J.; Chaban, G. M.; Gerber, R. B. *Chem. Phys. Lett.* **2000**, *331*, 308.
- (49) Aquilanti, V.; Luzzatti, E.; Pirani, F.; Volpi, G. G. *J. Chem. Phys.* **1988**, *89*, 6165.
- (50) Tarroni, R. *Chem. Phys. Lett.* **2003**, *380*, 624.
- (51) Sheng, L.; Gerber, R. B. *J. Chem. Phys.* **2007**, *126*, 021108.
- (52) Domanskaya, A.; Kobzareno, A. V.; Tsivion, E.; Khriachtchev, L.; Feldman, V. I.; Gerber, R. B.; Räsänen, M. *Chem. Phys. Lett.* **2009**, *481*, 83.

JP1001622